15 April 1994

ELSEVIER

Chemical Physics Letters 221 (1994) 53–58

CHEMICAL PHYSICS LETTERS

Resonance Raman and infrared spectroscopy of carbon nanotubes

J. Kastner [a], T. Pichler [a], H. Kuzmany [a], S. Curran [b], W. Blau [b], D.N. Weldon [c], M. Delamesiere [c], S. Draper [c], H. Zandbergen [d]

[a] *Institut für Festkörperphysik, Universität Wien, A-1090 Wien, Austria*
[b] *Department of Pure and Applied Physics, Trinity College, Dublin 2, Ireland*
[c] *Chemistry Department, Trinity College, Dublin 2, Ireland*
[d] *National Centre for HREM, Laboratory of Materials Science, Delft University, 2628 AL Delft, The Netherlands*

Received 26 November 1993; in final form 25 January 1994

Abstract

We present a comparative analysis of the vibrational and structural properties of carbon nanotubes. The first-order Raman spectrum exhibits two lines at 1582 cm^{-1} and at 1350 cm^{-1}. The observed ratio of the integrated intensity of these lines was found to be different as compared to polycrystalline graphite. The position and intensity of the line around 1350 cm^{-1} strongly depend on the energy of the exciting laser line. This dispersion effect is again different from the dispersion in nanocrystalline graphite. It is discussed in terms of a photoselective resonance process. Transmission infrared spectra of the nanotubes show one broad and asymmetric line at 1575 cm^{-1} and a weaker line at 868 cm^{-1}.

1. Introduction

Since the discovery of the successful production of buckminster fullerene in macroscopic quantities, worldwide attention has focused on the unique properties of these molecules [1]. The recent discovery of even larger fullerenes, graphitic nanotubes [2] and onion-like polyhedra [3], has substantially increased the interest in this area. These new carbon materials are interesting both from a scientific and technological point of view. There might be practical applications in such diverse areas as high tensile strength fibres, molecular wires and solenoids [4]. The basic structure of nanotubes consists of one or usually more graphitic sheets wrapped around one another with a hollow core. The caps are usually closed by the presence of carbon pentagons. Consequently, the tubes contain no dangling bonds. This is an intrinsic difference to graphite crystallites where open bonds are at the edges. Due to this difference and due to the curved nature of the graphitic sheets in the tubes characteristically different vibrational properties can be expected. However, the difference to the properties of graphite crystallites might be rather small since both materials are nanoparticles. Moreover, the deviation from planarity is low in the graphitic sheets of a typical tube with more than a few nanometer diameter.

Monocrystalline graphite belongs to the D_{6h}^4 space-group symmetry [5–9]. The irreducible representation for the zone center optical modes is given by

$$\Gamma_{opt} = 2E_{2g}\,(R) + E_{1u}\,(IR) + 2B_{2g} + A_{2u}\,(IR)\,. \tag{1}$$

The E_{2g} modes are Raman active. One is a shear-type rigid-layer mode at 42 cm^{-1} and the other an in-plane stretching mode at 1582 cm^{-1} often designated as the G mode. The infrared optical vibrations are an out-of-plane A_{2u} mode at 868 cm^{-1} and an in-plane E_{1u}

0009-2614/94/$07.00
SSDI 0009-2614(94)00234-H

mode at 1588 cm^{-1}. In polycrystalline graphite an additional line appears at 1350 cm^{-1} which can be assigned to phonons at the M and K points of the hexagonal Brillouin zone [5–7]. Since this line is disorder induced it is usually called the D line. Its second-order is of considerable intensity even in monocrystalline graphite because the phonon density of states has a maximum at 1350 cm^{-1}. Since the $k=0$ selection rule does not apply for second-order Raman scattering, phonons can be observed from any part of the Brillouin zone.

Raman spectra of carbon nanotubes [10] and closed-shell carbon particles [11] have been reported. A strong resemblance to the Raman spectrum of graphite was found. For carbon nanotubes the strongest Raman line is down-shifted by 6 cm^{-1} to 1574 cm^{-1} as compared to the E_{2g} mode of monocrystalline graphite. Additionally, a line at around 1350 cm^{-1} and its overtone at 2687 cm^{-1} have been observed.

In this Letter we present a correlation of the Raman spectrum of carbon nanotubes to their structural properties. Distinct differences between the resonance Raman behavior of carbon nanotubes, carbon microcrystallites and highly oriented pyrolytic graphite (HOPG) are discussed within a photoselective resonance picture. Finally, infrared (IR) spectra are presented and elucidated.

2. Experimental

The technique used to produce carbon nanotubes is similar to the one required for the production of fullerenes by using a steel fullerene generator. An 8 mm graphite rod of 99.99% purity and a plug of graphite were used as the positive and as the negative electrode, respectively. The generator was flushed with helium three times before evacuating to 450 Torr. A dc potential of 27 V was applied between the two graphite rods. After the positive electrode was consumed a cylinder with a grey outer layer and a black inner core was found on the negative electrode. This cylinder was placed in methanol and sonicated for ten minutes. This removed some of the inner black material from the cylinder to give a fine black suspension. After evaporating methanol a fine black powder was obtained containing approximately 70% nanoparticles of which nanotubes are by far the most abundant. This was proven by high-resolution electron microscopy (HREM). Due to the high tube concentration it can be assumed that the Raman spectra are dominated by lines from the tubes. The rest of the material consisted of a fused mixture of tubes and polyhedra, and of amorphous carbon. No graphitic crystallites were observed. The nanotubes showed a distribution in length and diameter. Evaluating the electron micrographs yielded a distribution as shown in Fig. 1. For the length an effective value is plotted where the graphitic planes are not interrupted by dislocations or breaks. Both values, the length and the diameter, show a bimodal distribution peaking at 30 and 70 nm and 60 and 180 nm for the diameters and for the lengths, respectively. More detailed results of the HREM measurements will be published elsewhere [12].

Raman spectroscopy was performed using a Dilor XY spectrometer with a liquid-nitrogen cooled CCD detector. As excitation sources Ar^+, Kr^+ and a Ti:sapphire laser with wavelengths ranging from 457 up to 742 nm have been used. The measurements were taken in back-scattering geometry with a typical laser power of 1 mW (140 W/cm^2) and a spectral resolution of 2–4 cm^{-1}. Line positions and widths were obtained from a numerical fit using Lorentzian

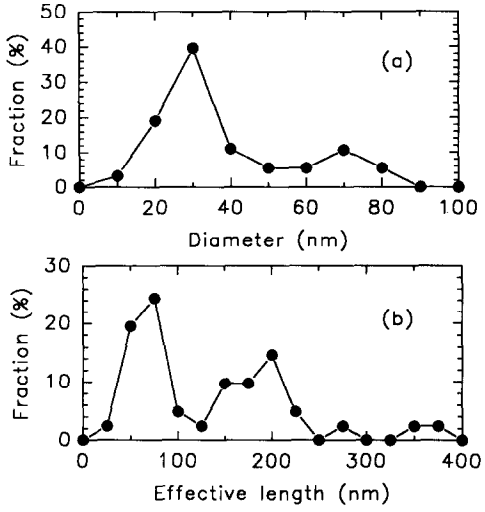

Fig. 1. Distribution in nanotube diameter (a) and effective length (b) as obtained by high-resolution electron microscopy. The total number of counted tubes was 350 and 60 for the diameter and the length, respectively.

line shapes. When conducting IR spectroscopy a mixture of 300 mg KBr and several milligrams of carbon nanotubes or graphite microcrystallites were prepared in pellet form. The pellets were placed in a Bruker IRS 66V spectrometer and transmittance spectra were taken between 400 and 5000 cm^{-1} with a resolution of 2 cm^{-1}. IR spectra of highly oriented pyrolytic graphite (HOPG) were taken from cleaved surfaces in reflexion 11° from normal incidence.

3. Results and discussion

3.1. Raman scattering

Fig. 2 shows Raman spectra in selected spectral regions of carbon nanotubes, graphite microcrystallites and HOPG after excitation with 457 nm. The strongest Raman line of all three studied materials has its maximum at 1582 cm^{-1}. It is the above mentioned G line. The full width at half maximum (fwhm) of this line is about 20–22 cm^{-1} for both nanotubes and graphite crystallites which is only slightly higher than that for HOPG (about 15–18 cm^{-1}). There is an additional line at 1350 cm^{-1} in the spectra of nanotubes and graphite microcrystallites assigned as the D line in Fig. 2. This line has the same intensity in both spectra.

The high-frequency part of the spectrum for all three materials studied is dominated by a strong line D* at around 2700 cm^{-1} which is the second-order of the D line. In the spectrum of HOPG this line consists of a doublet structure whereas in the other two

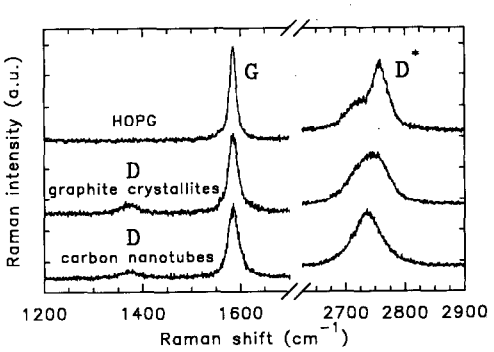

Fig. 2. Raman spectra of carbon nanotubes, graphite microcrystallites and highly oriented pyrolytic graphite (HOPG) as excited with 457 nm.

cases it is a single line. The D* line is much broader for crystallites (fwhm $\approx$ 71 cm^{-1}) and up-shifted (ν = 2742 cm^{-1}) as compared to nanotubes (fwhm $\approx$ 49 cm^{-1} and ν = 2734 cm^{-1}). In addition, there are several weak lines at 2455, 2955 and 3252 cm^{-1} in the second-order Raman spectra of all three materials. Since these lines are similar in shape and position for all studied materials they will not be discussed further. Raman lines at 100 and 860 cm^{-1} as calculated by Al-Jishi et al. [13] could not be observed. These new modes were predicted for tubes with a diameter of 2 nm. Since all observed tubes in our sample have a considerably large diameter, these additional Raman modes are expected to have vanishing intensity. In order to find the new nanotube modes future studies must concentrate on smaller tubes.

The D line is of considerable diagnostic significance because the ratio between its integrated intensity and the integrated intensity of the G line ($R = I_D/I_G$) depends on the structure of the studied carbon material. The in-plane graphite crystallite size L can be related to this ratio as [5–7]

$$L\,(\mathrm{nm}) = 4.4\,\frac{I_G}{I_D}\,. \qquad (2)$$

This relation is valid for $0.001 \leqslant R \leqslant 1$ and for laser excitation between 488 and 514 nm. Since in our case R is 0.23 and thus in the range of validity of Eq. (2) the latter gives a nanotube length of 20 nm. This is a factor of 3 or 9 lower than the average obtained from HREM for the two peaks in the bimodal distribution. Since the concentration of contaminants like polyhedra is very low in our samples, this discrepancy must have structural reasons. We suggest the curved nature of the graphitic layers leads to an enhancement of the D line due to an enhancement of the electron–phonon coupling. Since it is generally accepted that the electron–phonon coupling increases by a σ admixture to the sp^2 bonded carbon atoms the present explanation seems plausible. Applying this interpretation to lower and larger size tubes means that the intensity of the D line will decrease with increasing diameter of the carbon nanotubes and approach for big tubes the value known from polycrystalline graphite before it finally disappears.

There are two further parameters which correlate to the graphite crystallite size: the band widths of the

G and D* lines [5,7]. The smaller width of the D* line for tubes as compared to the one for crystallites is in accordance with the larger extension of the lattice along the direction of the tubes (nanotubes: $L = 130$ nm, graphite crystallites: $L = 20$ nm) and the enhancement of the D line for tubes due to their curved nature. From these considerations it can be concluded that the D* width versus crystallite size correlation is more or less identical for carbon nanotubes and polycrystalline graphite. However, the same width of the G line in both materials is at a first glance in contradiction to their different sizes. In order to understand it one has to take into consideration that the curved nature of nanotubes and their interplane disorder also lead to a line broadening. Hence the agreement of the widths for the G lines in tubes and in the crystallites is only by chance. The broadening mechanisms are completely different. The fact that only the G line for tubes and not the D* line is broadened might be related to the different origins of these lines. The G line is a zone center optical phonon, whereas the D* line is the second-order of a non-center phonon [7,9]. Calculations by Al-Jishi and Dresselhaus [9] showed that the low-energy side of the D* line dominantly comes from the K point and the high-energy side mainly from the M point. In the case of monocrystalline graphite and HOPG this gives a doublet structure with a shoulder at the low-energy side and in graphite crystallites a broadened single line. In carbon nanotubes the D* line is almost at the same position as the shoulder of the D* line for HOPG. Thus, for carbon nanotubes contributions from the region near a K derived point dominate the D* line due to the particular structure.

3.2. Resonance Raman scattering

In Fig. 3 Raman spectra of carbon nanotubes excited with different laser lines are shown. The spectra are normalized to equal height of the G line. Actually, the Raman intensity increases from $\lambda = 742$ nm to $\lambda = 457$ nm. The change of the signal to noise ratio originates from the spectrometer response function which has a broad maximum between 500 and 700 nm and is rather low at $\lambda = 457$ nm. One can clearly see that both the D and D* lines are shifted to lower wavenumbers with increasing wavelength of the exciting laser whereas the position of the G line remains constant. The down-shift of the D* line (89 cm^{-1}/eV) is about twice as much as the one of the D line (43 cm^{-1}/eV). This is good proof that the D* line is really the second-order of the D line. In addition, a new line at 1620 cm^{-1} appears in the spectrum after excitation with the yellow or red laser. This line was also observed in the spectrum of graphite crystallites and similarly to the D line it was assigned to disorder-induced symmetry breaking by the microscopic particle size [14,15]. As with the D line the phonon density of states has a maximum at this energy. For the case of the tubes the disorder originates from the finite tube size and thus the interpretation for the origin of the line corresponds.

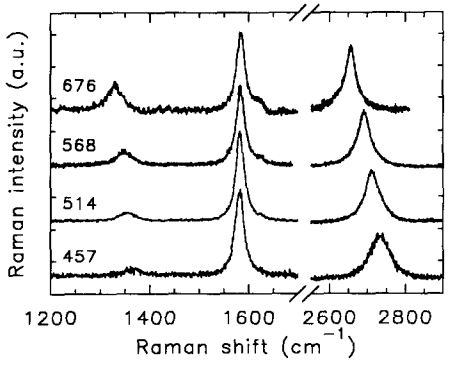

Fig. 3. Raman spectra of carbon nanotubes after excitation with different laser lines. The numbers indicate the wavelength in nm. The spectra were normalized so that the G lines have equal intensities in all cases.

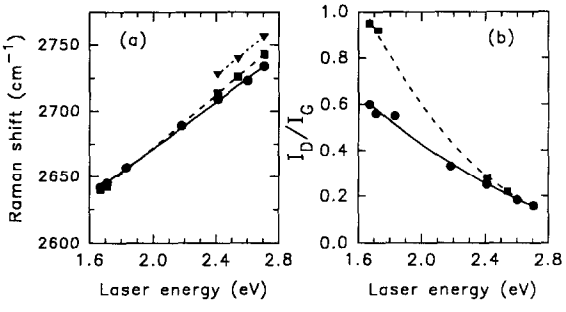

Fig. 4. Raman shift of the line around 2700 cm^{-1} (a) and integrated intensity of the D line as compared to the G line (b) for carbon nanotubes (●), graphite crystallites (■) and HOPG (▼) versus the energy of the exciting laser.

Fig. 4a shows explicitly the Raman shift of the D* line with the energy of the exciting laser line for all three studied samples. For HOPG only the position

of the high-energy line of the doublet is plotted. The D* line shift to higher wavenumbers is by about 15% weaker for carbon nanotubes as compared to graphite crystallites. The change of the relative intensities with the energy of the exciting laser is significant. The D line is much stronger as compared to the G line for excitation with the red laser as compared to excitation with the green or blue laser (Fig. 3). This is demonstrated in Fig. 4b. Here the intensity ratios of the D line to the G line are plotted versus the energy of the exciting laser for nanotubes and microcrystallites. This ratio decreases non-linearly with increasing laser energy and behaves characteristically different for tubes and graphite crystallites.

A dependence of the Raman shift of a mode on the energy of the exciting laser is formally called a dispersion effect. There are several possible explanations for this behavior.

It might be related to a probing of the sample at different depths below the surface as known from inorganic semiconductors [16]. This would require a depletion of carriers at the surface to the depth of the penetrating light. Since the tubes studied here are rather large they have a narrow electronic gap [4] and thus at room temperature a high carrier concentration. This situation is not compatible with a large depletion depth which consequently rules out this mechanism.

The dispersion might then be rather attributed to a photoselective resonance process. Two different mechanisms are possible for the tubes.

Similarly, as in conjugated polymers and sp-bonded linear carbon molecules [17–19] force constants, frequencies and electronic transitions may depend on the size of the nanotubes. By measuring with different laser energies one is probing selectively different parts of the sample and the overall response gives the resulting line shape and line position. Calculations showing an increase in the band gap with decreasing size for at least some of the tubes [4] are in agreement with this hypothesis. However, within this picture the independence of the line shift on the crystallite size is hard to explain. Therefore, another model may work better. The line shifting can be related to the dispersion of the D phonon at the Brillouin zone edge at the M and K derived points [14]. Excitations with different laser energies will result in different resonance enhancements of the contributions from regions near the K and M derived points to the D line.

In both photoselective resonance pictures the special electronic structure of carbon nanotubes accounts for the difference in the dispersion as compared to graphite.

A change in the I_D/I_G ratio with the energy of the exciting laser for different forms of polycrystalline graphitic materials was already observed by several authors [14,20,21]. It was attributed to a stronger resonance enhancement of the G line as compared to the D line [21]. By excitation with a red laser one is far away from the π–π^* transition (4–5 eV) and the G line is no longer more enhanced as compared to the D line. Applying this model to the results presented here reveals a difference in the resonance Raman profile for graphite and carbon nanotubes. This shows again that the electronic structure of carbon nanotubes is characteristically different from graphite and graphite microcrystallites.

3.3. Infrared spectroscopy

The IR spectra in selected spectral regions are shown in Fig. 5 for carbon nanotubes, graphite microcrystallites and HOPG. The spectra of nanotubes and microcrystallites have been measured in transmission using KBr pellets, whereas the spectrum of HOPG has been measured on an 11° tilted and cleaved surface in reflexion. For the presentation the background of all spectra was subtracted. This back-

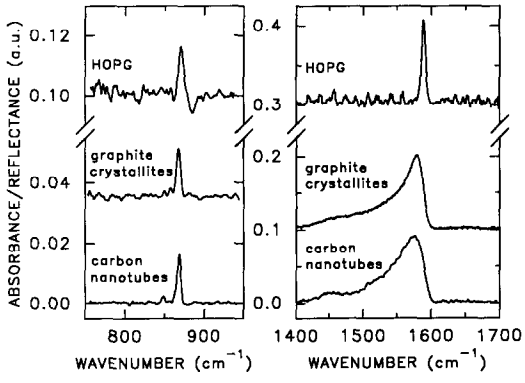

Fig. 5. Transmission infrared spectra in selected energy regions of carbon nanotubes and graphite microcrystallites. The infrared spectrum of HOPG measured in reflexion is included in the upper part of the figure.

ground was 100× larger than the line at 860 cm^{-1} and 1000× larger than the line at 1587 cm^{-1}.

The IR spectrum of HOPG shows the two known lines at 868 (A_{2u}) and 1587 cm^{-1} (E_{1u}), which is in good agreement with the results by Nemanich et al. [7,8]. The IR spectra for both carbon nanotubes and graphite crystallites are different from the one for HOPG, but resemble each other strongly. The A_{2u} mode is at the same position as in HOPG whereas the E_{1u} mode is softened to about 1575 cm^{-1} and considerably broadened with an asymmetric tail in the low-energy region.

The shift of the E_{1u} mode can have several reasons. Firstly, a change of the interplane bonding leads to a change of the E_{1u} line because its energy is associated with an interlayer force constant. Moreover, introduced disorder and finite size effects may lead to a line broadening and shifting as well. Finally, the bending of the graphitic sheets might lead also to the same effect. Probably all mechanisms contribute to the observed shape and position of the E_{1u} mode.

4. Conclusion

Carbon nanotubes have been characterized by high-resolution electron microscopy, resonance Raman and IR spectroscopy. It has been shown that the I_D/I_G ratio versus the in-plane graphite sheet size of carbon nanotubes is different from the corresponding relation in polycrystalline graphite. Due to the curved nature of the graphitic sheets the electron–phonon coupling constant and therefore also the D line is enhanced. A dispersion and resonance effect was found for the D line. The discrepancy between carbon nanotubes and graphite microcrystallites has been attributed to different resonance Raman profiles and their different electronic structure. IR spectra of carbon nanotubes have been presented. The difference to the spectrum of HOPG has been explained by disorder induced line broadening and softening.

Acknowledgement

This work was supported by the Osteuropa Förderung des BMfWF project GZ 45.212/2-27b91. We are grateful to D. John, Electron Microscope Unit, Trinity College, and R. Winkler, University of Vienna.

References

[1] W. Krätschmer, L.D. Lamb, K. Fostiropoulos and D. Huffmann, Nature 347 (1990) 354.
[2] S. Iijima, Nature 354 (1991) 56.
[3] D. Ugarte, Nature 359 (1992) 707.
[4] M.S. Dresselhaus, G. Dresselhaus and P.C. Eklund, J. Mater. Res. 8 (1993) 2054.
[5] D.S. Knight and W.B. White, J. Mater. Res. 4 (1989) 385.
[6] F. Tuinstra and J.L. Koenig, J. Chem. Phys. 53 (1970) 1126.
[7] N.B. Brandt, S.M. Chudinov and Ya. G. Ponomarev, Graphite and its compounds (North Holland, Amsterdam, 1988).
[8] R.J. Nemanich, G. Lucovsky and S.A. Solin, Solid State Commun. 23 (1977) 177.
[9] R. Al-Jishi and G. Dresselhaus, Phys. Rev. B 26 (1982) 4514.
[10] H. Hiura, T.W. Ebbesen, K. Tanigaki and H. Takahashi, Chem. Phys. Letters 202 (1993) 509.
[11] W.S. Bacsa, W.A. de Heer, D. Ugarte and A. Chatelaun, Chem. Phys. Letters 211 (1993) 346.
[12] D. Weldon, W. Blau, H. Zandbergen, S. Draper and M. Delamesiere, to be published.
[13] R. Al-Jishi, L. Venkataraman, M.S. Dresselhaus and G. Dresselhaus, Chem. Phys. Letters 209 (1993) 77.
[14] R.P. Vidano, D.B. Fischbach, J. Willis and T.M. Loehr, Solid State Commun. 39 (1981) 341.
[15] K. Nakamura, M. Fujitsuka and M. Kitajima, Phys. Rev. B 41 (1990) 12260.
[16] G. Abstreiter, M. Cardona and A. Pinczuk, in: Light scattering in solids, Vol. 4, eds. M. Cardona and G. Güntherodt (Springer, Berlin, 1984).
[17] H. Kuzmany, Phys. Stat. Sol. b 97 (1980) 521.
[18] H. Kuzmany and J. Kastner, in: Macromolecules 1992, ed. J. Kahovec (VSP, Zeist, 1993) 333.
[19] J. Kastner, H. Kuzmany, L. Kavan, F. Dousek and J. Kürti, J. Chem. Phys., submitted for publication.
[20] T.P. Mernagh, R.P. Cooney and R.A. Johnson, Carbon 22 (1982) 39.
[21] K. Sinha and J. Menendez, Phys. Rev. B 41 (1990) 10845.